Supporting Information

# Optical voltage sensing using DNA origami

*Elisa A. Hemmig,[†§] Clare Fitzgerald,[†§] Christopher Maffeo,[¥] Lisa Hecker,[†] Sarah E. Ochmann,[φ] Aleksei Aksimentiev,[¥] Philip Tinnefeld,[φ] Ulrich F. Keyser*[†]*

[†]Cavendish Laboratory, Department of Physics, University of Cambridge, JJ Thomson Avenue, Cambridge, CB3 0HE, United Kingdom, [§]E. A. Hemmig and [§]C. Fitzgerald contributed equally. [¥] Institut für Physikalische und Theoretische Chemie, TU Braunschweig, 38106 Braunschweig, Germany, and Department for Chemistry and Center for Nanoscience, Ludwig-Maximilians-Universität München, 81377 München, Germany.

*Corresponding Author Email: ufk20@cam.ac.uk; Phone number: 01223 337272

**Contents**

1. Agarose gel of purified DNA origami structure.

2. AFM image of the DNA-tile structure.

3. Description of the model construction protocol and the model parameters.

4. Experimental setup for combined single-molecule FRET and ionic current measurements.

5. Bulk fluorescence emission spectra of DNA origami structures.

6. Voltage-dependent properties of the DNA origami plates.

7. Simultaneous fluorescence and ionic current measurements.

8. Response of dye intensities to change in voltage.

9. Proximity Ratio response of origami designs to electric field, immobilised on capillaries with starting inner and outer diameters of 0.3 mm and 0.5 mm respectively.

10. Proximity Ratio response of origami designs to electric field, immobilised on capillaries with starting inner and outer diameters of 0.2 mm and 0.5 mm respectively.

11. Further example traces of the change in the Proximity Ratio $E_{sm}^{*}$ for a single trapped origami structure.

12. Estimated force required to stretch the dsDNA leash.

13. Scaffold-staple layout for the DNA origami structure and staple strand sequences.

14. Diagram of PDMS-based micro-fluidic chip.

15. Analysis of occurrence of single vs. multiple origami trapping events.


Animation 1: Capture of the origami plate between 100 and 400 mV.

Animation 2: Translocation of the plate under high bias.

Animation 3: FRET pair distance in captured plate.
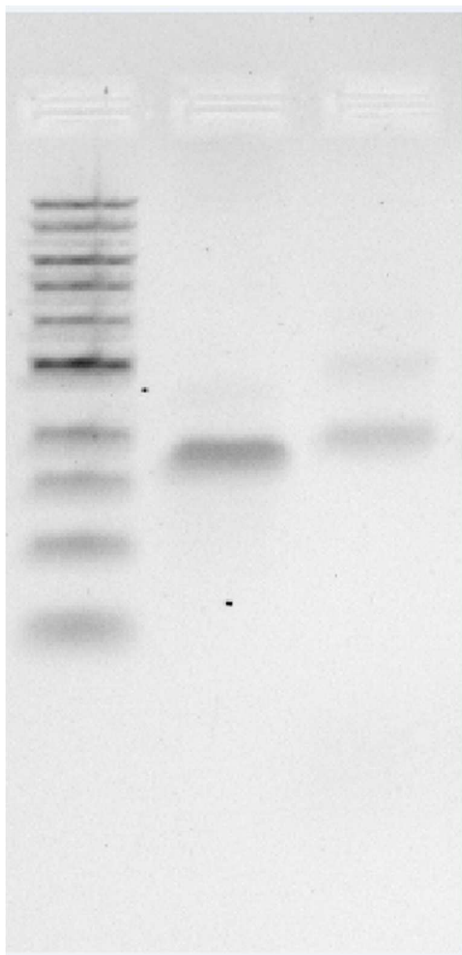
1. **Agarose gel of purified DNA origami structure.**



**Figure S1.** Agarose gel electrophoresis (1%) of DNA origami plates performed in 11 mM $MgCl_2$ buffered with 0.5x TBE. Lane 1: 1 kb ladder, Lane 2: p8064 scaffold, Lane 3: DNA plate with leash and pore (p8064) (from left to right).
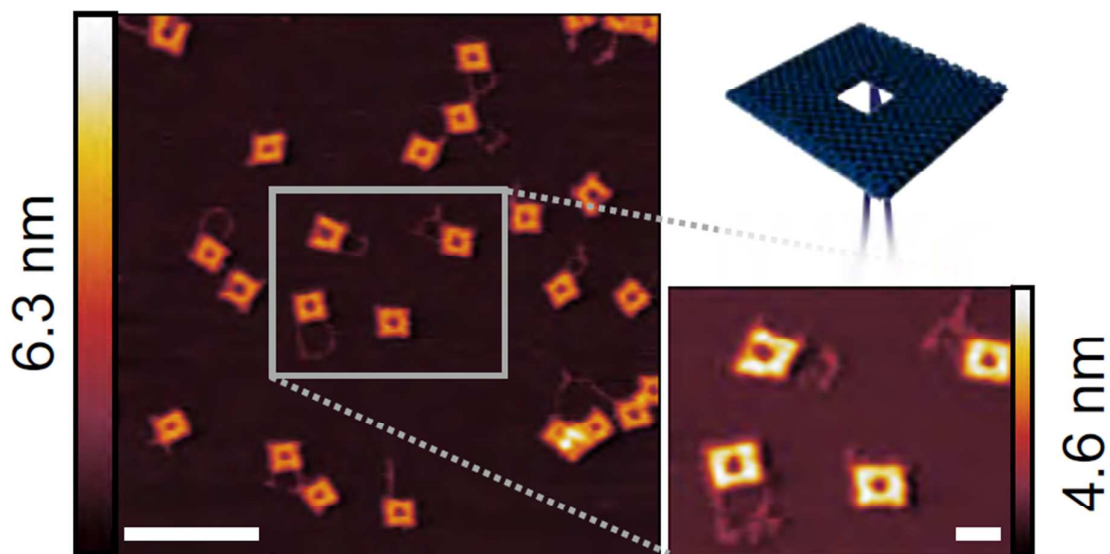
## 2. AFM image of the DNA-tile structure.



**Figure S2.** AFM image of purified DNA origami plates. AFM was performed in air. The scale bars correspond to 250 nm and 50 nm (inset image). The approximate lateral DNA origami plate dimensions extracted from AFM height profiles are 50.6±2.5 nm (±SD) and 55.1±2.2 nm (±SD), the height 3.1±0.2 nm (±SD), and the central pore dimensions 15.4±0.6 nm (±SD) and 16.1 ±0.5 nm (±SD). Each size was determined from analysing 5 individual structures.

### 3. Description of the model construction protocol and the model parameters.

Simulations were performed under various applied bias potentials. For each voltage, a spatially varying electrostatic potential was obtained from a continuum COMSOL multiphysics model that solved coupled equations for incompressible Stokes flow, electrostatics, and Fick's diffusion of ions. The COMSOL model is described in detail below. The resulting electrostatic potential was exported in a three-dimensional grid used to apply forces to the DNA using an effective charge of 0.25 $e$ per nucleotide, where $e$ is the fundamental charge of an electron. This scaling factor is consistent with experimental measurements of the effective force due to an applied bias on a DNA molecule in a nanopore of similar geometry to the nanocapillary.[1] Simulations were performed using a cut-off of 40 Å and integration timesteps of 200 and 50 fs for low- and high-resolution models, respectively. The diffusion coefficient of each bead was set to 150 Å$^2$/ns and the temperature was set to 291 K.

**Continuum model of a nanocapillary.** A continuum model of the nanocapillary was constructed using the COMSOL multiphysics software package. Specifically, the modules "Creeping flow", "Transport of diluted species", and "Electrostatics" were used to model the electric potential in and around the pore. The outer diameter of the capillary was set to 2.5 times the inner diameter. At the aperture, the inner diameter was 10-nm. Between the aperture and a 100 nm distance along the capillary axis, the inner diameter increased with a 5.2° slope from the axis. Between 100 nm and 5000 nm, the slope decreased to 2.7° from the axis. Boundary conditions were set that prevented flow outside the nanocapillary between 500 and 1000 nm along the capillary axis as measured from the aperture. The overall system dimensions were 15000 nm along the capillary axis, and 2000 nm across. The bulk concentration of KCl solution was set to 1 M. The steady state solution to the coupled system

of equations was solved numerically at 1 atm and 298.15 K using the azimuthally-symmetric 2D projection of cylindrical coordinates.

The equations for incompressible Stokes flow were solved with solvent density of 1 g/cm$^3$, and viscosity of $8.9 \times 10^{-4}$ Pa s, with no slip boundary conditions on all walls except the surfaces representing the entrance and exit of the chambers above and below the capillary, where the pressure was set to zero. A volumetric force was applied to the fluid with $-F (c_{+} - c_{-}) V$, where $F$ is the Faraday constant, $c_{\pm}$ is the local concentration of ions, and $V$ is the local electrostatic potential. The electrostatic potential was calculated according to the Poisson equation given a distribution of ions with a relative permittivity of 80, no charge boundary condition on the walls of the *cis* and *trans* chambers, a surface charge of $-0.01$ C/m$^2$ on the glass capillary, and variable voltage difference across the chambers. Finally, the ion concentration was determined by a system of equations that allowed convection coupling to the solvent flow, diffusion using $D = 1.9579 \times 10^{-5}$ and $2.032 \times 10^{-5}$ cm$^2$/s, and the electrostatic force on the charged particles, using a mobility $\mu = D/k_B T$.

The resulting electric potential was rotated azimuthally and exported in a regular $240 \times 240 \times 950$ voxel grid at a resolution of 0.5 nm in the directions normal to the capillary axis, and 0.2 nm along the capillary axis. The exported region contained 40 nm beyond the aperture of the capillary and 150 nm of the capillary. The potential within the nanocapillary walls was set to 20 kcal/mol providing a steric barrier. The potential map was then smoothed by convolution with a 1-nm wide three-dimensional Gaussian kernel.

**Construction of the coarse-grained model.** A low-resolution model of the object was constructed using a python script that directly queried caDNAno data structures. A coarse-grained bead was first placed at every crossover and at the ends of each ssDNA or dsDNA segment. Within each caDNAno helix, additional beads were placed at evenly spaced positions between adjacent pairs of the crossover or terminal beads so that fewer than seven

base pairs or four ssDNA nucleotides would be located between any pair of beads. Harmonic intrahelical bond potentials were placed between the dsDNA beads with a rest length of 0.34 × $N_b$ nm/bp or 0.5 $N_b$ nm/nt and with $k_{spring}$ = 10/$N_b$ or 1/$N_b$ kcal mol$^{-1}$ nm$^{-2}$ for dsDNA and ssDNA, respectively, where $N_b$ is the number of base pairs or nucleotides between the beads. A harmonic potential was placed on the angle between every three consecutive beads within a helix with rest angle of 180° and $k_{spring} = \frac{1.5}{1-e^{-N_a/N_p}}$ k$_B$T radian$^{-2}$, where $N_a$ is the number of base pairs or nucleotides between the first and third bead and $N_p$ is the persistence length expressed in base pairs or nucleotides, 147 and 3 for dsDNA and ssDNA, respectively.

Crossover bonds were defined by harmonic potentials having the rest length of 1.85 nm and $k_{spring}$ = 4 kcal mol$^{-1}$ nm$^{-2}$, matching observations from simulations.[2] A harmonic potential was also applied to the angle between the connected crossover beads and each adjacent crossover bead on the same double-helical segment. The potential was assigned a rest angle of 90° and $k_{spring} = \frac{0.75}{1-e^{-N_c/N_p}}$ k$_B$T radian$^{-2}$, where $N_c$ is the number of basepairs between the crossovers. Another harmonic potential was applied to the dihedral angle between each set of four beads forming adjacent crossovers within a double helical segment with rest angle of 34.2°/bp offset by ±120° if the crossovers occur between strands with opposing sense. The spring constant for the dihedral angle potential was determined using a least squares fit so that

$$\langle\cos(\varphi)\rangle = \int_0^{2\pi} d\varphi \, \cos(\varphi) \, e^{-\frac{k_{spring}\,\varphi^2}{2\,k_BT}} \Big/ \int_0^{2\pi} d\varphi \, \cos(\varphi) \, e^{-\frac{k_{spring}\,\varphi^2}{2\,k_BT}} = e^{-N_c/N_{tw}} \qquad (1)$$

where $N_{tw}$ = 265 is the twist persistence length expressed in terms of base pairs.

We extracted the potential of mean force per turn between parallel, effectively infinite DNA helices from all-atom umbrella sampling simulations as previously described, except the electrolyte contained 100 mM MgCl$_2$.[3] This potential was used as a target for refinement of the non-bonded interactions between the coarse-grained beads. Two parallel, idealized

helices were constructed, allowing the per-turn coarse-grained interaction potential to be calculated by integrating a trial bead–bead interaction potential over the lengths of DNA. With the value of the bead–bead potential at each 0.1 nm from 0 to 5 nm taken as a variable, the coarse-grained helix interaction was optimized against the all-atom potential of mean force using a least-squares protocol. This process was repeated for all pairs of coarse-grained bead sizes, where the size of each bead was taken to be half of its intrahelical bond lengths when express in terms of nucleotides. Pairs of beads connected by fewer than seven intrahelical bonds were excluded from nonbonded interaction calculations. Also excluded were nonbonded interactions between each crossover bead and the partner crossover bead in the adjacent helix and the two nearest neighbour beads of the partner bead.

The high-resolution model was constructed in the same manner as the low-resolution model described above, except that beads were placed at a density of 1 bead/bp. In addition, a dummy azimuthal orientation bead was added to each dsDNA bead, connected through a stiff harmonic bond with rest length of 1 Å and $k_{\text{spring}} = 30$ kcal mol$^{-1}$ Å$^{-2}$. Each adjacent pair of dsDNA beads had harmonic potentials placed on the angle between each orientation bead and the two dsDNA beads with rest angle of 90° and $k_{\text{spring}} = \frac{0.75}{1-e^{-N_{\text{b}}/N p}}$ $k_{\text{B}}$T radian$^{-2}$. Finally, a dihedral angle potential was placed between the orientation bead, its parent dsDNA bead, the adjacent dsDNA bead and its orientation bead with a rest angle of 34.2°/bp and $k_{\text{spring}} = 110$ $k_{\text{B}}$T/radian$^2$. Hence the orientation bead provided a measure of the local twist of the DNA and interacted with the rest of the system only through the above bonded terms.

The initial coordinates of the high-resolution model were obtained by mapping onto the coordinates of the low-resolution model as follows. Each high-resolution non-orientation bead was placed by interpolating the position of the two nearest intrahelical low-resolution beads at the end of the simulation. The orientation beads were placed with 1-Å offset, normal to the axis of interpolation and with a 34.2°/bp twist. Specifically, the azimuthal angle for the

orientation bead was obtained from a quaternion-based interpolation of the rotation matrices minimizing the mean square deviation between initial and final coordinates of the neighbourhoods around the adjacent low-resolution beads in the same helix. The neighbourhood for each bead of the low-resolution model was taken to be all beads within 5 nm and beads in the same helix within 10 nm of the bead.

**Simulation of the coarse-grained model.** All simulations employed the Atomic Resolution Brownian Dynamics software package.[4] Every time step $\tau$ (200 and 50 fs for low- and high-resolution models, respectively), the force $F_i$ on each particle was evaluated and the positions were updated as $\Delta x_i = \frac{D\tau}{K_B T} F_i + \sqrt{2 D \tau} R$, where $D = 1.5 \times 10^{-5}$ is the diffusion coefficient of each bead, and $R$ is a vector of random numbers pulled from a normal distribution. The temperature was set to 291 K. For the force evaluation, a non-bonded cut-off of 4 nm and a non-bonded pair list distance of 12 nm were used, allowing update of the pair list just every 100000 integration steps. The force on each bead due to the capillary was taken to be the negative gradient of the potential, scaled by 0.25 times the number of nucleotides in the bead. The factor of 0.25 was previously found to provide the effective electrophoretic force on a DNA molecule in a nanopore of similar geometry.[1]

The low-resolution model of the DNA origami plate was placed about 10 nm above the nanocapillary with the leash initially compacted and facing the capillary aperture. For each applied bias, a 40 µs simulation was performed, during which capture of the plate occurred. Capture occurred quickly at all applied biases, except in the 100 mV case. The capture simulation was therefore extended for another 40 µs for 100 mV.

The conformation of the system every 2 µs during the last 10 µs of the capture simulation was used to construct a series of high-resolution models for each applied bias. For each configuration, a 2 µs simulation yielded the distance between base pairs that had fluorescent dyes attached, providing an estimate for the distance between the FRET dye pairs.

## 4. Experimental setup for combined single-molecule FRET and ionic current measurements.
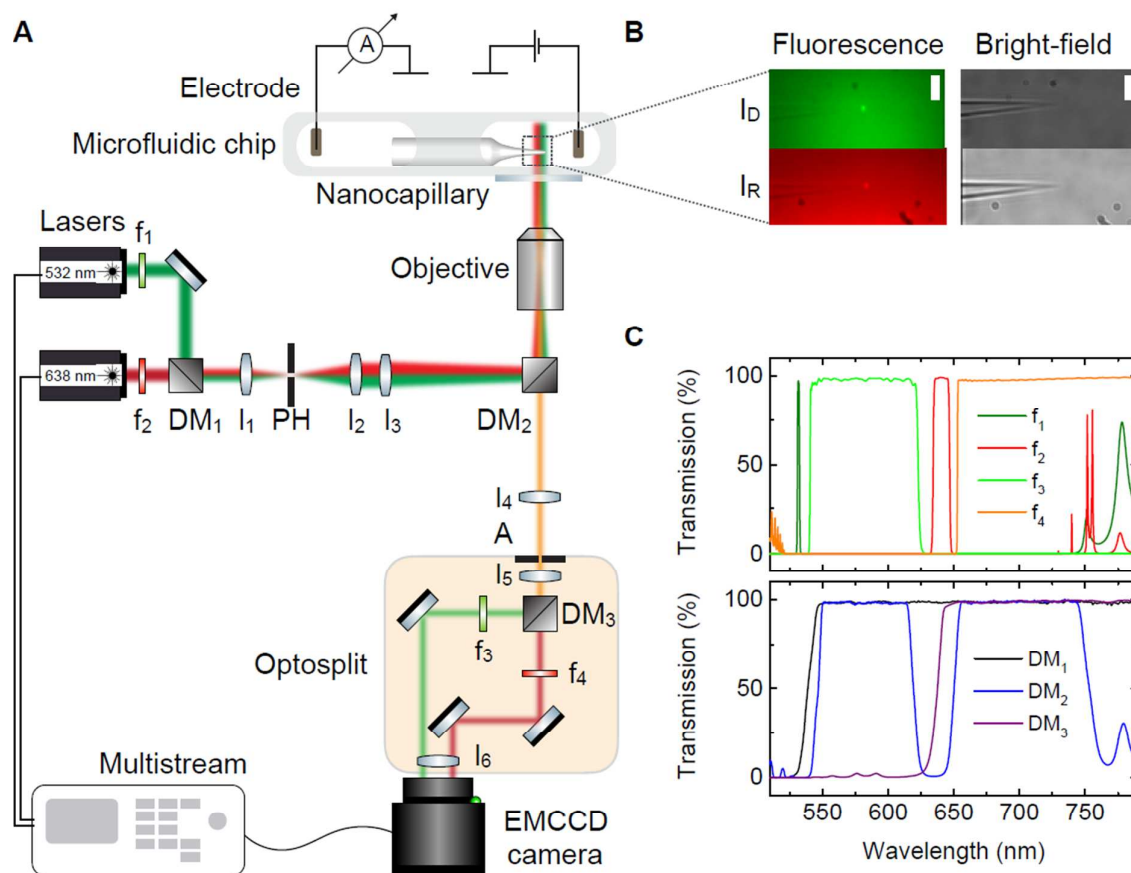


**Figure S3:** Experimental setup for combined single-molecule FRET and ionic current measurements. **A** Schematic of the inverted fluorescence microscope with wide-field illumination and two colour alternating laser excitation (ALEX). The main optical components are the green and red lasers, the microscope objective (60x), the Optosplit, the EMCCD camera, the Multistream device, optical filters ($f_{1-4}$), lenses ($l_{1-6}$), dichroic mirrors ($DM_{1-3}$), a pinhole ($PH$), and a rectangular aperture $A$. The two laser beams are combined by a dichroic filter $DM_1$ (Omega Optical 540DRLP). A dual-edge dichroic beamsplitter $DM_2$ (Semrock FF545/650-Di01) acts as a wavelength specific filter separating excitation and emission light. The emission light is separated into its two spectral bands using a Cairn OptoSplit II device. The core of the Optosplit is a dichroic beamsplitter $DM_3$ (Chroma T635lpxr), which separates the 'green' and 'red' spectral components of the emission light at a 635 nm cut-off. The two beams are further spectrally purified using a 582/75 nm BrightLine® single-band bandpass

filter $f_3$ (Semrock FF01-582/75) and a 647 nm RazorEdge® ultra-steep long-pass edge filter $f_4$ (Semrock LP02-647RU). A microfluidic chip hosting the nanocapillary is located above the objective. Electrodes are immersed into the electrolyte chambers and enable application of a voltage across the nanocapillary for ionic current recordings. **B** Field of view in fluorescence and bright-field mode. The imaging area is split into two spectral channels ($I_D$ and $I_A$) that are spatially equivalent. The fluorescence image is averaged over 914 frames acquired at 20 Hz with alternating laser excitation. The spots in the green and red fluorescent channels represent a fluorescent DNA origami structure trapped on the nanocapillary tip. The contours of the nanocapillary are clearly visible in the bright-field image. Scale bar 5 $\mu$m. **C** (*top*) Transmission spectra of optical filters $f_{1-4}$. (*bottom*) Transmission spectra of dichroic mirrors $DM_{1-3}$ at an incident angle of 45°. Illustrations of the optical components were partially taken from the Component Library by Alexander Franzen.

## 5. Bulk fluorescence emission spectra of DNA origami structures.

The bulk fluorescence properties of the DNA origami designs $A_1$ and $A_2$, each labelled with a FRET pair (ATTO532 and ATTO647N) were determined by steady-state fluorescence emission measurements in solution (Figure S4). We excited the donor dye ATTO532 at a wavelength of 500 nm and the acceptor dye ATTO647 at a wavelength of 600 nm. Upon donor excitation, the emission in the wavelength range 530-600 nm ($I_D(D^*)$) can be attributed to the donor while emission in the spectral window 635-700nm ($I_A(D^*)$) corresponds to acceptor emission due to FRET. For acceptor excitation, we measure direct acceptor emission in the spectral window 635-700 nm ($I_A(A^*)$). We can use these fluorescence intensities to obtain the proximity ratio $E_{ens}{}^*$

$$E_{ens}^* = \frac{I_A(D^*)}{I_D(D^*) + I_A(D^*)} \tag{2}$$

for both DNA origami designs $A_1$ and $A_2$. This results in $E_{ens}{}^* = 0.200\pm0.01$ for design $A_1$ and $E_{ens} = 0.073\pm0.01$ for design $A_2$. The errors are the standard deviation of the mean. $E_{ens}$ is a factor of 2.6 larger in design $A_1$ compared to $A_2$, which is consistent with the shorter inter-dye separation in design $A_1$ vs. $A_2$.
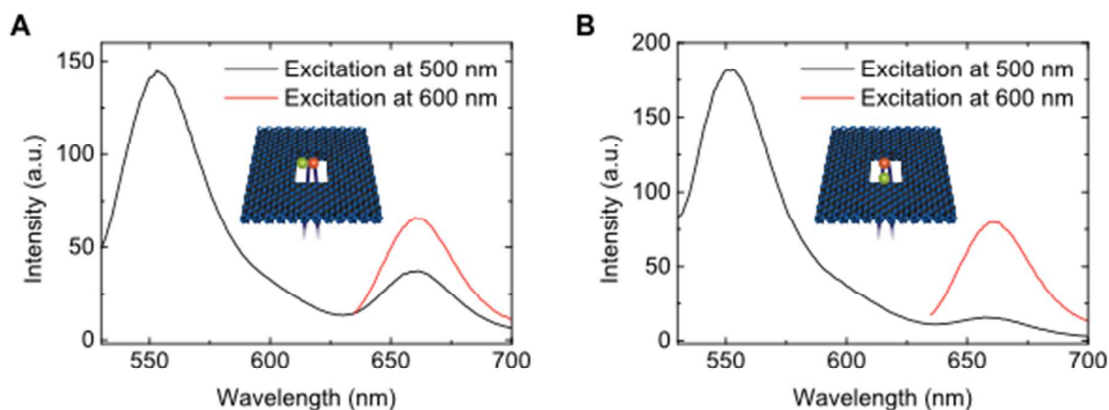


**Figure S4. A** Fluorescence emission spectra measured in bulk of DNA origami design $A_1$ when excited at 500 nm (*black*) and excited at 600 nm (*red*). **B** Fluorescence emission spectra measured in bulk of DNA origami design $A_2$ when excited at 500 nm (*black*) and excited at 600 nm (*red*).

## 6. Voltage-dependent properties of the DNA origami plates.

Stable trappings of the origami structures occurred at voltages between 100 mV and 400 mV. The capillaries that showed stable trappings over this entire voltage range were found to have a bare capillary resistance lying within 31-40 MΩ.

A summary of the voltage-dependent properties of DNA origami plates with pore and a 260 nm long double-stranded leash is shown in Figure S5. Representative histograms of the relative conductance change $\Delta G$ at voltages ranging from 100 mV to 300 mV are shown in Figure S5A. At low voltages (100-200 mV), there is a single population of $\Delta G$, which can be attributed to the conductance state with a smaller current drop ('state 1'). This distribution shifts towards higher $\Delta G$ values as the voltage increases. At 250 mV and 300 mV, a distinct second population appears with a larger current drop ('state 2'). This second conductance state refers to the buckled conformation resulting from plastic deformation of the DNA origami plate. Evidence for this buckled conformation has been observed in our previous work.[5]
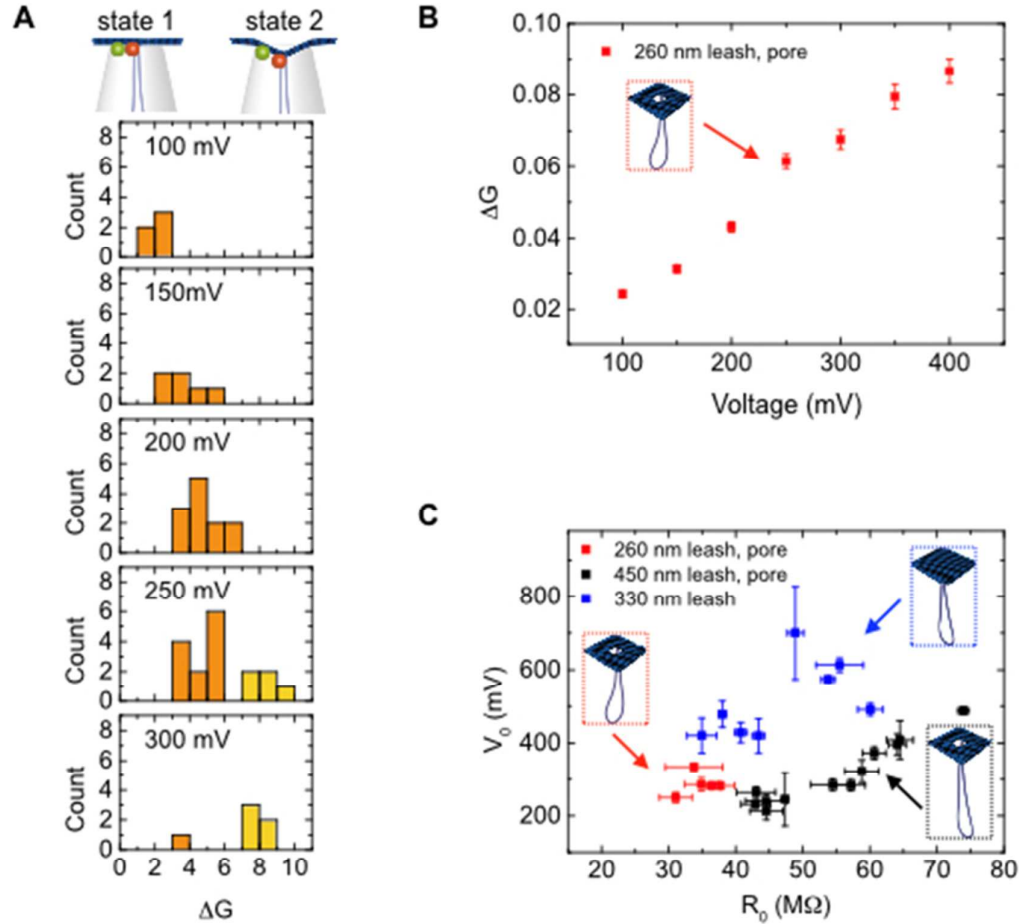
**Figure S5:** Voltage-dependent properties of DNA origami plate with pore and 260 nm leash. **A** Representative histograms of relative conductance change $\Delta G$ at various voltages (100 mV-300 mV). Two conductance states (state 1 in *orange* and state 2 in *yellow*) appear at voltages higher than 200 mV. **B** Average $\Delta G$ due to trapping of DNA origami plate (pore, 260 nm leash) as a function of the voltage applied. The measurements were carried out in 500 mM KCl, 5.5 mM MgCl$_2$ buffered with 0.5x TBE (pH ~8.6). The error bars correspond to the standard error of the mean. **C** Comparison of the relationship two-state voltage $V_0$ vs. estimated inner nanocapillary diameter $d_i$ for different DNA origami structures. The 260 nm leash, pore structure (*red*) was measured in 500 mM KCl and the 450 nm leash, pore (*black*) and the 330 nm leash, pore (*blue*) structures were measured in 1 M KCl. The error bars correspond to the standard deviation.

**7. Simultaneous fluorescence and ionic current measurements.**
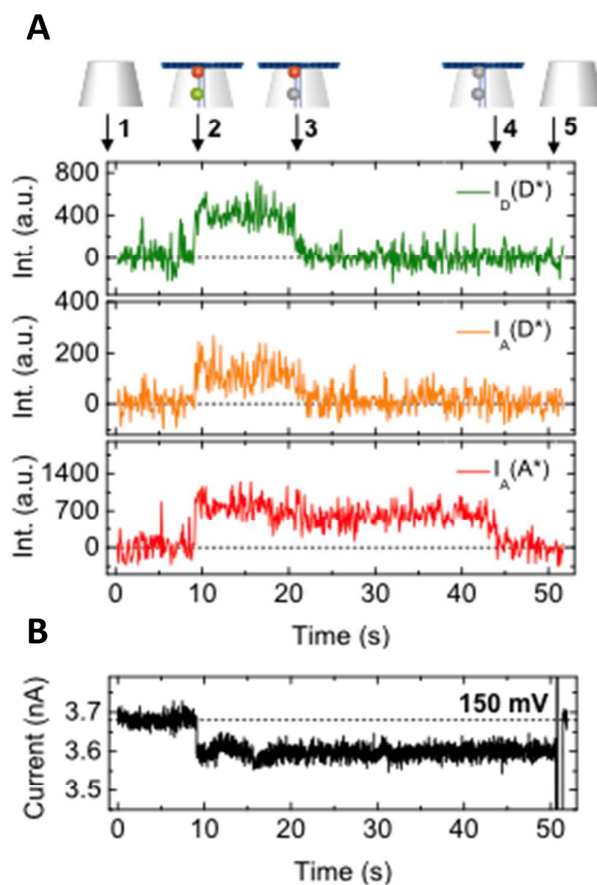


**Figure S6.** Representative example of fluorescence intensity traces correlated with voltage and ionic current recordings for DNA origami plates with design $A_2$. **A** (*top*) Trace annotations: 1 Bare capillary. 2. DNA origami trapped. 3 Donor bleaching. 4 Acceptor bleaching. 5 DNA origami ejection. (*Bottom*) Fluorescence intensity traces $I_D(D^*)$, $I_A(D^*)$, $I_A(A^*)$. The ATTO532 dye bleaches after ~20s preventing further FRET, shown by the loss of the $I_A(D^*)$ signal at ~20s. The ATTO647N dye bleaches after ~45s. **B** Ionic current trace at 150 mV.

**8. Response of dye intensities to change in voltage.**
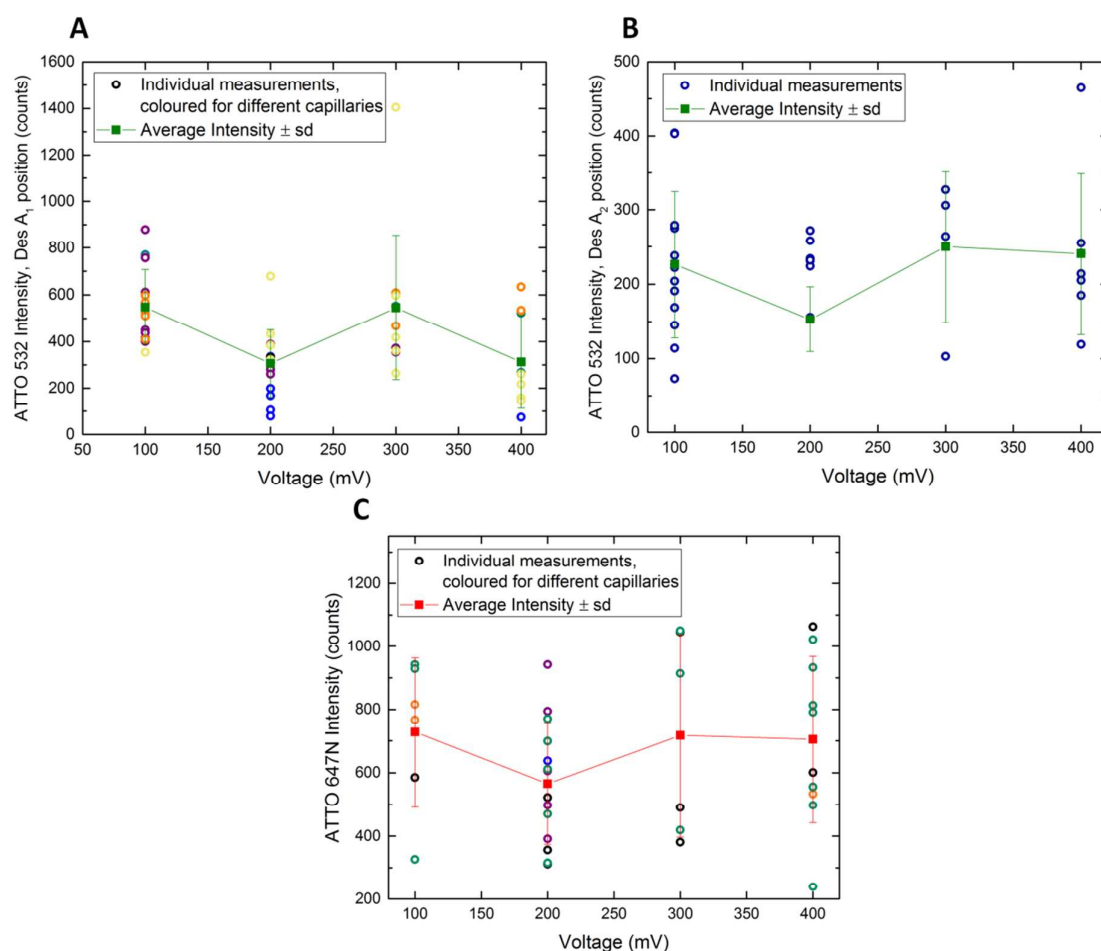


**Figure S7:** Dye intensities for ATTO532 (A and B, for dye positions in designs $A_1$ and $A_2$ respectively) and ATTO647N (C) when exposed to voltages ranging from 100 to 400 mV. Measurements were taken using the origami designs folded with single dyes only to remove the influence of quenching and FRET on fluorescence intensity. The individual intensity values (*open circles*) were obtained by averaging the intensity over the period of time the origami was immobilised on a nanocapillary tip. Different coloured circles refer to different nanocapillaries which will have varying properties such as resistance and height above the objective. The individual intensity values have also been averaged for each voltage. There is no systematic change in intensity with voltage observed implying negligible influence on the dye photo-physics by the surrounding voltage.

9. **Proximity Ratio response of origami designs to electric field, immobilised on capillaries with starting inner and outer diameters of 0.3 mm and 0.5 mm respectively.**



**Figure S8:** Change in Proximity Ratio $E_{sm}^*$ as a function of the voltage applied for design $A_1$ and $A_2$. We used $N_{tot} = 185$ traces from 8 capillaries in design $A_1$ and $N_{tot} = 241$ traces from 6 capillaries in design $A_2$. The error bars correspond to the standard error of the mean. Taking an average over all the voltages, the proximity ratio $E_{sm}^*$ is considerably higher in design $A_1$ ($E_{sm}^* = 0.53 \pm 0.08$ (SD)) than in design $A_2$ ($E_{sm}^* = 0.22 \pm 0.01$ (SD)). This is consistent with the theoretical inter-dye distances, which are shorter in design $A_1$ ($R_1 = \sim 3$ nm) than in design $A_2$ ($R_2 = \sim 5.8$ nm). At low voltages (100-200 mV), $E_{sm}^*$ lies between 0.57 to 0.62. Above this voltage range, $E_{sm}^*$ decreases in a linear fashion at $\Delta E_{sm}^* / \Delta V \approx 0.1/100$ mV. In contrast, for design $A_2$, where the donor and acceptor are positioned along the double-stranded leash, the proximity ratio $E_{sm}^*$ stays constant over the entire voltage range 100-400 mV at ~0.22.

**10. Proximity Ratio response of origami designs to electric field, immobilised on capillaries with starting inner and outer diameters of 0.2 mm and 0.5 mm respectively.**
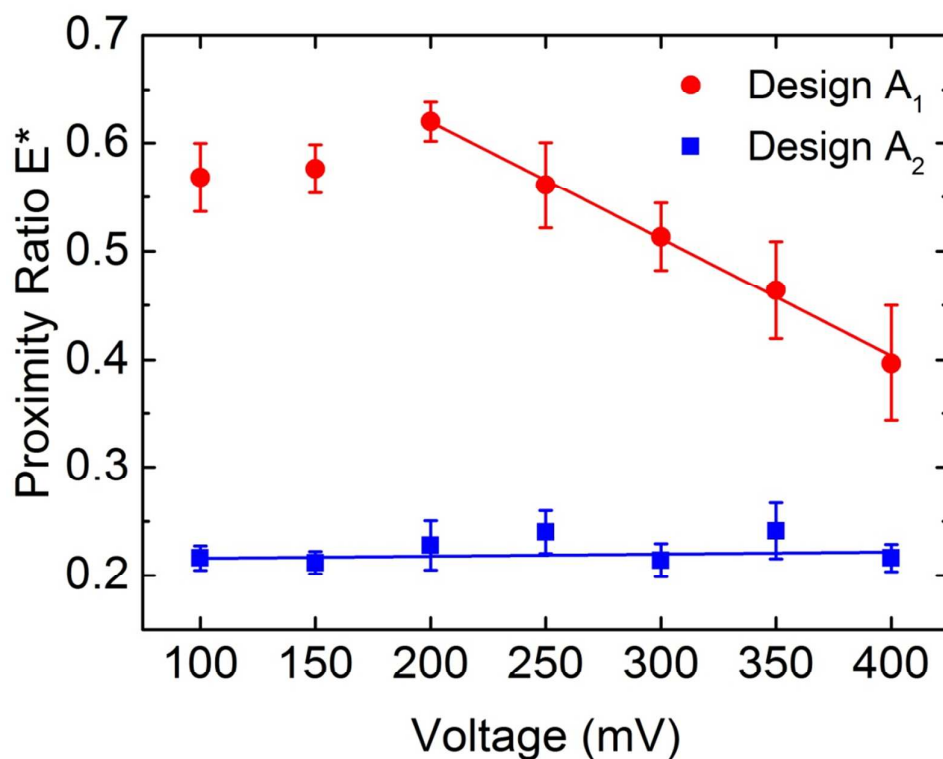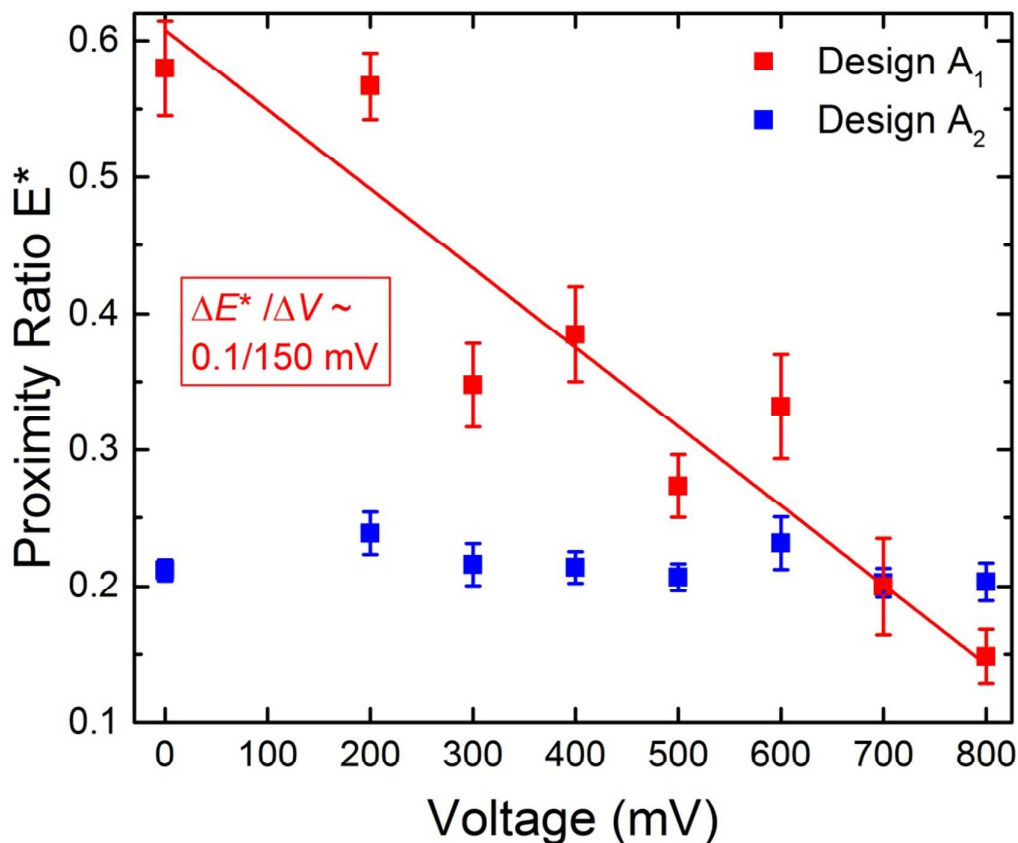


**Figure S9:** Proximity Ratio $E_{sm}{}^*$ as a function of the voltage applied for design $A_1$ and $A_2$. Capillaries have starting inner and outer diameters of 0.2 and 0.5 mm respectively. Stable origami trapping voltages ranged from 200 to 800 mV. We used $N_{tot} = 226$ traces from 69 capillaries in design $A_1$ and $N_{tot} = 144$ traces from 38 capillaries in design $A_2$. The error bars correspond to the standard error of the mean. Analogous to using capillaries with the larger inner diameter of 0.3 mm, a decrease in the proximity ratio with increasing voltage is observed for design $A_1$ but not for design $A_2$.

**11. Further example traces of the change in the Proximity Ratio $E_{sm}{}^*$ for a single trapped origami structure.**
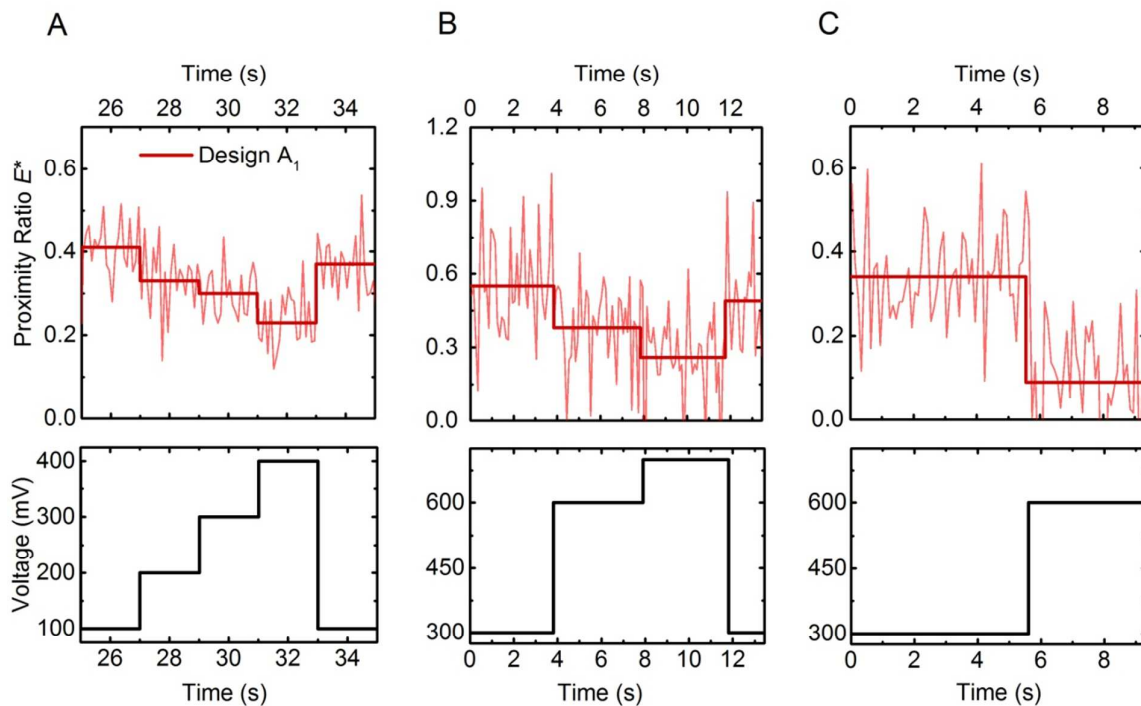


**Figure S10.** Further example traces (*top*) of the change in proximity ratio $E_{sm}{}^*$ for a single trapped origami structure (measured and average trace for each voltage step) with steps in voltage (A - 2 seconds, $\Delta V = 100$ mV; B – 4 seconds, $\Delta V = 300, 100$ mV; C – 4 seconds, $\Delta V = 300$ mV) for design $A_1$. Measurements are for capillaries with starting inner diameters of 0.3 mm (A) and 0.2 mm (B, C).

## 12. Estimated force required to stretch the dsDNA leash.

The elastic behaviour of dsDNA has been extensively characterised,[6] giving rise to three broad force-extension regimes: Entropic elasticity at low forces (~0.1-10 pN), intrinsic elasticity at intermediate forces (~5-50 pN) and overstretching at high forces (>65 pN).[7,8] As the persistence length of dsDNA is $l_p \approx 50$ nm,[8] a leash section of length 6 nm will be straight at room temperature. Within our voltage range of 100-400 mV, we estimate an upper force limit of roughly 16 pN per DNA molecule (assuming the electric force normalised by the voltage applied on a DNA molecule in a nanopore is $\kappa \approx 0.04$ pN/mV).[5,6,9] We will thus consider the intrinsic elasticity regime to estimate what force $F$ is needed to stretch a 17 bp long dsDNA polymer such that its end-to-end distance $x$ exceeds its theoretical B-form contour length $L$. Based on the approximation[7]

$$\frac{x}{L} = 1 - \frac{1}{2}\left(\frac{k_B T}{F l_p}\right) + \frac{F}{S}$$

(3)

and using a stretch modulus $S = 1000$ pN,[7] we obtain $F > 40$ pN for $x/L > 1$ at room temperature. Hence, the range of electric forces applied in our experiment are all far below the minimum force required to induce a linear elastic response of the stiff leash section connecting the FRET pair in design $A_2$.

**13. Scaffold-staple layout for the DNA origami structure and staple strand sequences.**
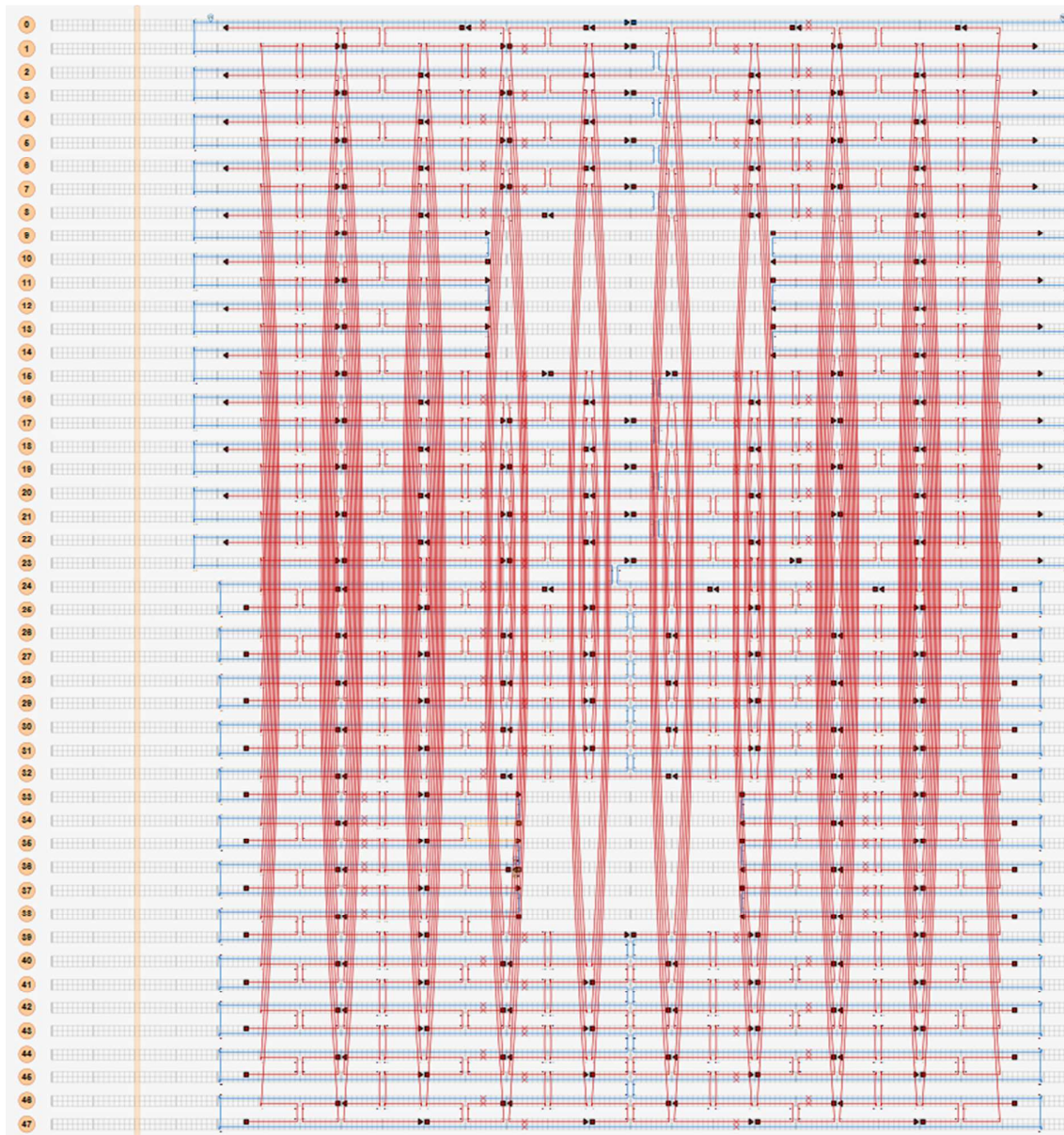
Below is the staple list of the DNA sequences for all unfunctionalised staples. The staples contributing to the leash are marked in red and the staples with biotins attached to the 5' end for surface measurements are highlighted in yellow.

| Start | End | Sequence (5' to 3') |
|---|---|---|
| 15[56] | 34[56] | GATGATGGTTATCATTTGAGCGCGAAACAA |
| 20[167] | 25[167] | CATTCAGGGATCGCACGGCTATCAGAAAAGCC |
| 0[175] | 45[167] | GAACAAGAGTCCACTAGAAATCGGGTGTCGAAAACGGTGT |
| 35[72] | 13[84] | AGTTACCACCAATAATCCGAACGTTATTA |
| 37[72] | 11[84] | AAGAGGCTTCAGTGCCATATCTTTAGGAG |
| 30[55] | 15[55] | AACGCTAAACAAAATAAGATTTTCGATTATCA |
| 44[55] | 1[55] | TTAAACAGCAACCATCGGTTGCTTACGTGGCG |
| 31[168] | 18[168] | GAGCTGAAATTAACATCTTTCTCCCCAAGCTT |
| 27[72] | 22[72] | TTCCTTATTATCAACAGTAAATGCCTGACCTA |
| 24[186] | 21[191] | ATTTAAATTGTAGGAAGATCAAACGGCGCTTTCCGGCACCGCT |
| 4[167] | 41[167] | ACTCACATAATTCCACGAACTGGCGAGATTTA |
| 34[186] | 11[191] | AGAGAGTACCTAAACTCCACAAGAATGCATTGCAGGCGCTTTC |
| 1[88] | 47[103] | CGCTAGGCGTGAACCACGAAGGCACCAACC |
| 28[87] | 17[87] | GTTTTTACTCCCGACGAAGATGGCTTTGAA |
| 47[72] | 2[72] | AATACGTAAGACAGCAAAGCGAAAGCGCCGCT |
| 25[136] | 23[143] | CATATGTAAATTTTTGCTGGCCTT |
| 23[112] | 26[120] | ACGCCATCAAAAATAAGTAACCGTAACTAGCAAGAATCGA |
| 22[71] | 24[56] | AATTTAATAGCCTGTTCGCCATATTTAACAAC |
| 3[88] | 46[88] | GAACGGTCCCGCCGCGGCTTGCACCCTCAG |
| 17[56] | 32[56] | AAACAATAAATTGCGTAACAGCCAGAAGCGCA |
| 4[103] | 41[103] | TGAGGCCACAGCCATTTCGTCTTTTTAGCGTA |
| 12[167] | 33[167] | AGCACCGTGCCGGACTTCCTTTTGTGTAGCTC |
| 1[152] | 47[167] | GTGGTTCCTTAAAGAACCCAGCGATTATACCA |
| 42[151] | 3[151] | CCAGTCACGAGTAGTTTGCGCTGGCCAACG |
| 8[135] | 40[120] | GACGATCCAGCGCAGTTAGCGAGAACCAGACG |
| 29[136] | 20[136] | TACCAAAATGAGTAATAAAGGGGGGAAGGGCG |
| 37[168] | 12[168] | GGTCTTTATGCATCAAAGCGGGGTCCAACGGC |
| 29[72] | 20[72] | TAGCGAACTTTTCATCTGAATAACTAAGACGC |
| 46[55] | 0[33] | AACGGCTAAGGAAGTTTGCCGTAAAGCACTAAATCGGAA |
| 25[37] | 23[55] | TCGAGCCAGTAGTAATTTAACCGGAATCATAATTA |
| 11[56] | 38[56] | AGGAAGGTAACCTCAAAAACATGTGCTCAG |
| 27[37] | 22[33] | CGAGCATGTAGATAATATCCCTCCGGCCGTGTGATAAATAAG |
| 46[151] | 0[144] | CCTGCTCCTTTGACCCGTGGAC |
| 17[88] | 32[88] | TACCAAGAAATTATTGAAACGAGCCTTTAC |
| 2[135] | 43[135] | GCAGCAAGCTGCATTGTAACAAACGAGAAA |
| 38[55] | 7[55] | TACCAGGCATAGCCCGACCAGCAGGAGATAGA |
| 27[168] | 22[168] | TGATAAATTCTACAAATCCAGCCAGGATTGAC |
| 38[90] | 7[87] | AGAGAAGGATTGAGGTTTAAAACATCAATACGTG |
| 46[186] | 0[176] | TATCATCGCCTACAAAGTACCAGTTTG |

| | | |
|---|---|---|
| 28[119] | 18[104] | AAAAGGGTAGAGCATACGGAATTATTCATTTC |
| 32[87] | 33[90] | AGAGAGAACCCACAAGAA |
| 2[103] | 43[103] | CCACCACAACGCCAGAAGCCTTTACTCCAAAA |
| 17[152] | 32[152] | ATTTGTGAATTTCTGCTTTTCATTCAGTTGAT |
| 1[56] | 47[71] | AGAAAGGAGGTCGAGGTCCATTAAACGGGTAA |
| 39[168] | 10[168] | AAAATGTTTCATAAATCATCCCTTGGTATGAG |
| 32[119] | 15[119] | GACCATTAAAAAATGACTGAATAATGGAATCG |
| 44[87] | 1[87] | GGTTTATGTCGCTGAGCTTAATGGAGCGGG |
| 17[112] | 32[120] | AGGCGCGAAACGTACAGGTTGTGTTCGCAAATTTTAGTTT |
| 28[151] | 17[151] | CAATGCCACATTATGCACGGGAGTCCCGGA |
| 9[139] | 40[152] | TGGGTAAAGGTTTCTTTGCTCCGGTGCCGCAGAGGGGAGTAAGAG |
| 33[37] | 16[33] | AACAAAGTCAGGAGAATTAATATTCCTAGGTTTAACGTCAGA |
| 26[151] | 19[151] | CCTGAGAAATATGATCTGTTGGATGTGCTG |
| 6[167] | 39[167] | AGCCTCCTGCGGGCCGCGAGGCATGTAATAGT |
| 25[72] | 23[87] | AAAGGTAATTGAGAATTAGTATCATATGCGTT |
| 41[104] | 7[111] | ACGATCTAACCCTCAGTTGAATGG |
| 35[37] | 14[33] | CCTTTTTAAGACAATAGCTAACAATTCCAAAGAAACCACCAG |
| 46[87] | 0[80] | CAGCGAAATGCCACTATCACCC |
| 29[104] | 19[111] | AAGCCTTAGCACTCATTTAATTAA |
| <mark>19[56]</mark> | <mark>30[56]</mark> | <mark>AATCAATAGAAAACAAAGAACGCGATCTTACC</mark> |
| 21[152] | 28[152] | CTCAGGAACTGCGCAAATTCAACCTTTAAATG |
| 37[37] | 12[33] | TTCGGAACCTACAGTTAATCAGTTGAATACATTTGAGGATTT |
| 6[71] | 39[71] | GGATTATTGACCTGAATTCAGGGAGTATCACC |
| 2[167] | 43[167] | TTGCCCTTGAGGCGGTCAAGAACCCTTGAGAT |
| 26[119] | 20[104] | TGAACGGTGAGAAAGGTCGCCTTAGAATCCTT |
| 32[55] | 13[55] | TTAGACGGAGGGTAATTTGCGGAAGACAACTC |
| 18[103] | 27[103] | AATTACCTCGTCGCTACGAGAACATATTAAAC |
| 3[112] | 46[120] | AAGTGTGTCGTGCCAGCGGTCCACAAGGGAACAACGAGGC |
| 2[71] | 43[71] | ACAGGGCGGCCGATTATTTCGAGGTTGCGAAT |
| 33[168] | 16[168] | AACATGTTGTTTCATTTGAAGGGTAGCGGATC |
| 26[55] | 19[55] | CAAGAAAAAAACCAATTGAATTTAAGTACATA |
| 41[72] | 8[72] | CATTCCACCCCTCATTAGCGTAAGGCCATTAA |
| 20[71] | 25[71] | TGAGAAGAAACTATATATAGATAATACCGACA |
| 23[56] | 26[56] | CTAGAAAAGGTTTGAAATATAAAGGTCCTGAA |
| 40[55] | 5[55] | CCAATAGGCAGTACAACAGATTCAACTCAAAC |
| 15[152] | 34[152] | AGGCGGCCGCTGGCAGATAATGCATAAGAG |
| 21[56] | 28[56] | GGTTATATGTCAATAGCAATAATCCATTACCG |
| <mark>5[56]</mark> | <mark>44[56]</mark> | <mark>TATCGGCCTAACCGTTTAAAGGAATGAATTTC</mark> |
| 5[88] | 44[88] | TTACCGCCCGAGTAATGAAAATATTGTATC |
| 29[37] | 20[33] | AGGCTTATCCGAGCAAGCAATGGAAACTCAAAATCATAGGTC |
| 19[112] | 30[120] | TTTTCCTATTACGCCAGAAACAATAAGCTAAATAAGCAAT |
| 45[168] | 4[168] | ACAGACCAAATCTTGATTGCGTATGTGAGCTA |
| 46[119] | 0[104] | GCAGACGGAAGAGGCAGTCTATCAGGGCGATG |
| 34[55] | 11[55] | TGAAATAGAAAGTAAGATAGATAAAGGAATTG |
| 30[87] | 15[95] | ACCCAGCCCAAATAATGCACGTTCCTGATTGTTTGGA |
| 19[88] | 30[88] | TGTAAATGAGCAAAATTGCGGGTATTTTGC |

| | | |
|---|---|---|
| 16[103] | 29[103] | CCATATCATTACAAAATTAGTTGCAGGTTTTG |
| 34[90] | 35[90] | TTGAGTTAAGCGAAGGAAACCG |
| 43[37] | 6[33] | GAGAATAGAAATTTCAACAGTAGAAGACCAGTCACACGACCA |
| 5[112] | 44[120] | AAAAAATGGTCATAGCGTCGGGAATGCCCTGAGCTGCTCA |
| 34[151] | 12[139] | GTCATTTTTTCGAGCTCCATCCCACGCAA |
| 0[103] | 45[103] | GCCCACTAGCGCTGGCGGATCGTCAGGGAGTT |
| 43[136] | 6[136] | CACCAGAAGGACGTTGTGTGTGAACCGGGTAC |
| 1[112] | 47[135] | CGGTCGGTTTGCCCCAGAAAAACCAAAGAATACACTAAA |
| 45[136] | 4[136] | ACCAACTTAAATCAACAATGAATCCACTGCCC |
| 16[135] | 29[135] | AGTTGGGCGCGCCATAGCAAAATTCGGTTG |
| 8[95] | 40[88] | TAGCCCTAGTACCGCCCCTCAGA |
| 30[151] | 15[151] | GCAAGGCTAGCTATATCATTTGAGCCGCAC |
| 41[168] | 8[168] | GGAATACCAGGAATTATTTTCACGGGTTACCT |
| 18[167] | 27[167] | TCAGAGGTTTAAGTTGTCATATATGTTCTAGC |
| 40[151] | 5[151] | CAACACTGAAAGATTAGGATCCATTGTTAT |
| 12[84] | 33[71] | CACTAACAACTAATAGATTAGTCCTTTGCAAGAGCAATAATATCA |
| 7[112] | 42[120] | CTATTACTGCGCGCCTAATTCGTAACGGAACAAATCTACG |
| 47[168] | 2[168] | AGCGCGAAGATAAATTCAAAATCCACAGCTGA |
| 7[152] | 42[152] | AGAATGCGCACAGTTGCATCAGTTTCATTATA |
| 35[168] | 14[168] | CCGGAAGCTTAATTGCTGTAGAACGTTTTTTC |
| 36[151] | 10[139] | GCCCGAAAGAATGACCCTGCGGCTGGTAA |
| 20[103] | 25[103] | GAAAACATCGCAAGACAGCTAATGACGACGAC |
| 42[186] | 3[190] | TTACCTTATGCTTCAACTTCCTAATGATGGGCGCCAGGGTGG |
| 31[37] | 18[33] | ATTTGCCAGTTCGAGCGTCCCTTTTACACATTTAACAATTTC |
| 39[112] | 8[96] | AACCAAAAGTCAGTCTTTAATGCGCGAACTGA |
| 36[88] | 37[90] | TTAACGGGGGAGACTCCTCA |
| 15[96] | 31[103] | TTATACTTAAATAGCATTTTTTGT |
| 24[55] | 21[55] | GCCAACATATAAGAGAATACCGACTTAGGTTG |
| 41[37] | 8[33] | AGTTTCGTCACAACCCATGGGCCAACAAAGATAAAACAGAGG |
| 4[135] | 41[135] | GCTTTCCATGTTTCCGGAAGAAAACATTAT |
| 3[56] | 46[56] | AACAGGAGCGTACTATGCCCACGCAGGGTAGC |
| 6[135] | 39[135] | CGAGCTCGGTGCACTCCTCGTTTGGCTTTT |
| 40[119] | 6[104] | ACGATAAAACGAACTAATCCGCTCATGGAAAT |
| 33[72] | 16[72] | GAGAGATAATAACATACAATATAAAAAACAGA |
| 10[84] | 35[71] | ATCTAAAGCATCACCTTGCTGTATCTAAATTGAGTAACCGAACAA |
| 21[88] | 28[88] | ATCCAATAGCGATAGGAACGGGAGCAAGCC |
| 8[71] | 37[71] | AAATACCGAGAGCCAGCGGGGTTTAAAGTATT |
| 0[79] | 45[71] | AAATCAAGTTTTTTGGAGGGAAGATCGGAACGATAACCGA |
| 44[186] | 1[190] | TCATCAAGAGTGGCGCATAGACGGGCACTTATAAATCAAAAG |
| 41[136] | 8[136] | TACAGGTAATCATAACCTGTGGTGCTGCATCA |
| 22[103] | 23[111] | TATATTTTTTCTTACCAGTATGGA |
| 15[120] | 31[135] | ACATAAAAAAATCCCCGAGTAGAGGTCAAT |
| 28[55] | 17[55] | CGCCCAATGTATTCTAAATTAATTATCGGGAG |
| 36[55] | 9[55] | CGTATAAATTATTCTGATATCAAACAACAGTG |
| 7[56] | 42[56] | ACCCTTCTTACATTGGACTACAACGATTTTGC |
| 19[152] | 30[152] | CAAGGCGAGGAGCCGCACCCTGTATCATACAG |

| | | |
|---|---|---|
| 24[159] | 21[151] | TTAAAAATTCGCATTACCCCGGTTACGTTGGGTATCGGC |
| 10[167] | 35[167] | CCGGGTCACCAGCATCAAAGATTAGAACCAGA |
| 18[135] | 27[135] | CCTCACCGGCTGGCGGTGTAGGTAGTCAAA |
| 31[136] | 18[136] | AACCTGTTAAAGAATTGTTTACCAACGGATAA |
| 37[133] | 36[133] | TCAGAAAACGAGACTTCAAATA |
| 45[72] | 4[72] | TATATTCGCAGCTTGCAAGGGATTTGTCCATC |
| 36[186] | 9[191] | GCAAAGCGGATCCCTGACTGCGGTTGCACACTGGTGTGTTCAG |
| 5[152] | 44[152] | CCGCTCACTAATTGCGAAATTGGGGGATATTC |
| 33[133] | 16[136] | TAGAGCTTAATTCTGCGAAGTAAAAAACCGCCAGC |
| 44[119] | 2[104] | TTCAGTGATCAATCATGCTACGCTGCGCGTAA |
| 39[136] | 38[133] | GCAAAAGACTTTAAACAGT |
| 39[72] | 9[84] | GTACTCAGAGGATTAGCAGCAAATGAAAA |
| 30[119] | 16[104] | AAAGCCTCGATACATTACAGGGTTAGAACCTA |
| 14[167] | 31[167] | GTCTCGTCTTTAGTGACCATATAATGGGGCGC |
| 31[104] | 17[111] | TTAACGTCAATCAAGATCGCGCAG |
| 29[168] | 20[168] | GCGGGAGATAGAACCCGGTAACGCCCATTCGC |
| 22[135] | 24[128] | GGCGCATCTTCGCGTTTAAATCA |
| 42[55] | 3[55] | TAAACAACGGAACAACGTAGCAATGGGAGCTA |
| 7[88] | 42[88] | GCACAGATTTGACGCCTCATAGCCAGACGT |
| 47[104] | 1[111] | TAAAACGACTTTTGCGAAGTGTAG |
| 18[71] | 27[71] | AACATCAATATGTGAGGTAGGAATGGCTGTCT |
| 43[72] | 6[72] | AATAATTTTGAATTTTAATATCCATCTGAAAT |
| 14[84] | 31[71] | ATTTTAAAAGTTTGAGTAACACAATTCATAAAACAGGTATTATTT |
| 27[104] | 21[111] | CAAGTACCACATGTTCAAAGAACG |
| 25[168] | 23[191] | CCAAAAACAAACGTTATAAATGTGAGCGAGTAACAACCCG |
| 44[151] | 1[151] | ATTACCCTGAAAGAGGGCCCTGGTTTGATG |
| 24[95] | 21[87] | AACAGTAGGGCTTAAAGTAATTCTCATCTTTGATGCAA |
| 4[71] | 41[71] | ACGCAAATTTGCTGGTCTGTATGGGCCTGTAG |
| 45[37] | 4[33] | GACAATGACAACTTGATACATCAGAGCACTTCTTTGATTAGT |
| 38[151] | 7[151] | CTCAAATGAGTTTTGCGTGCCCCCTGCGGCC |
| 20[135] | 25[135] | ATCGGTGCGAGGGGACAAACAAGTGTCAAT |
| 47[37] | 2[33] | ACTTTTTCATGCAGAGGCTGCCGGCGATGACGAGCACGTATA |
| 42[119] | 4[104] | TTAATAAAATAAGGCTACCTTTTTATAATCAG |
| 23[88] | 26[88] | ATACAAAAGTTAATTTGTCCAGCAGAACGC |
| 6[103] | 39[111] | ACCTACATCAATATTTAACCGCCACACCCTCAGAACCGCC |
| 11[139] | 38[152] | CCAGCTTACGGCTGGAGGTGTCTGTTGCCATAAATCAATCCCC |
| 16[71] | 29[71] | AATAAAGAACGGATTCTATCCTGAAGGCGTTT |
| 16[167] | 29[167] | AAACTTAAGAGATAGACCAATAAAATACTTTT |
| 24[127] | 22[104] | GCTCATTTTTTAACCAAATCGTAAGCAAAACTTTTTCAAA |
| 43[104] | 5[111] | AAAAGGCTAAGTTTTGGCAACAGG |
| 3[152] | 46[152] | CGCGGGGACACCGCCTGACAGATGATCCGCGA |
| 8[167] | 37[167] | GCAGCCAGGTCATAAAATTCATTGAAAAATCA |
| 45[104] | 3[111] | AAAGGCCGCCAAAAGGATCCTGAG |
| 25[104] | 24[96] | AATAAACAATAAAAGCCAACGCTC |
| 26[87] | 19[87] | GCCTGTTCATTCCAACTTAGATCTTGCTTC |
| 21[112] | 28[120] | CGAGATCTGCCAGTTTGGGCCTCTCCGGAGACAAAGATTC |

| | | |
|---|---|---|
| 38[186] | 7[190] | CTGCGGAATCGTAGACTGGAGATGCCGGTCATACCGGGGGTT |
| 30[186] | 15[191] | ATAGTAGTAGCAAGGTGGCGCAGAAACAAAGTTAAACGATGCT |
| 32[186] | 13[191] | GGTGTCTGGAATTAAATATCGCGGTCCGTCAGCGTGGTGCTGG |
| 40[87] | 5[87] | GCCACCAAGACAGCCTCAATCGGAACAATA |
| 47[136] | 2[136] | ACACTCATCATGTTACAAAATCCTAGAGAGTT |
| 40[186] | 5[190] | ATAACGCCAAAACATTCAAGTTCTTCGCGAGCCGGAAGCATA |
| 13[139] | 36[152] | CACATCCTCATAACGGAACGTCGGTGGTGTCAAAGCAGAGGAA |
| 9[56] | 40[56] | CCACGCTGAACGAACCGAATAGGTTAGCAAGC |
| 32[151] | 14[139] | TCCCAATTGCTGAATCCTCCGGCCAGAG |
| 27[136] | 22[136] | TCACCATCGTCTGGAGCGACGACATGTAGATG |
| 26[186] | 19[191] | TTTTTGAGAGATAATGCCGGCAAAGCGCAGGGTTTTCCCAGTC |
| 43[168] | 6[168] | GGTTTAATGATTTTAAACAACATACGTCCGTG |
| 22[167] | 24[160] | CGTAATGGATCAACATATATTTTG |
| 23[144] | 26[152] | CCTGTAGCCAGCTTTCGATAGGTCGATAATCAGGTCATTG |
| 13[56] | 36[56] | GTATTAAAAGCCGTCACAGATAGCAGTGCC |
| 28[186] | 17[191] | ATAAAAATTTTAGCCTTTAGGCCAGTGGTGGTGAAGGGATAGC |
| 42[87] | 3[87] | TAGTAAATTTCACGTAAGAGTCTTAGACAG |
| 31[72] | 18[72] | ATCCCAATTACAATTTGCCTGATTATGAAACA |
| 35[133] | 34[133] | TCGCGTTTTAATGCGGATGGCT |
| 39[37] | 10[33] | TTGATATAAGTGGATAAGTACCGCCTGCCCTCAATCAATATC |
| 0[143] | 45[135] | TCCAACGTCAAAGGGCGCAGGCGTTAGCCGGCGAACTG |
| <span style="color:red">36[90]</span> | <span style="color:red">36[89]</span> | |
| | <span style="color:red">leash1</span> | <span style="color:red">AGGAAACGCAATAATAACGGAATACCCAAAAG</span> |
| | <span style="color:red">leash2</span> | <span style="color:red">AACTGGCATGATTAAGACTCCTTATTACGCAG</span> |
| | <span style="color:red">leash3</span> | <span style="color:red">TATGTTAGCAAACGTAGAAAATACATACATAA</span> |
| | <span style="color:red">leash4</span> | <span style="color:red">AGGTGGCAACATATAAAAGAAACGCAAAGACA</span> |
| | <span style="color:red">leash5</span> | <span style="color:red">CCACGGAATAAGTTTATTTTGTCACAATCAAT</span> |
| | <span style="color:red">leash6</span> | <span style="color:red">AGAAAATTCATATGGTTTACCAGCGCCAAAGA</span> |
| | <span style="color:red">leash7</span> | <span style="color:red">CAAAAGGGCGACATTCAACCGATTGAGGGAGG</span> |
| | <span style="color:red">leash8</span> | <span style="color:red">GAAGGTAAATATTGACGGAAATTATTCATTAA</span> |
| | <span style="color:red">leash9</span> | <span style="color:red">AGGTGAATTATCACCGTCACCGACTTGAGCCA</span> |
| | <span style="color:red">leash10</span> | <span style="color:red">TTTGGGAATTAGAGCCAGCAAAATCACCAGTA</span> |
| | <span style="color:red">leash11</span> | <span style="color:red">GCACCATTACCATTAGCAAGGCCGGAAACGTC</span> |
| | <span style="color:red">leash12</span> | <span style="color:red">ACCAATGAAACCATCGATAGCAGCACCGTAAT</span> |
| | <span style="color:red">leash13</span> | <span style="color:red">CAGTAGCGACAGAATCAAGTTTGCCTTTAGCG</span> |
| | <span style="color:red">leash14</span> | <span style="color:red">TCAGACTGTAGCGCGTTTTCATCGGCATTTTC</span> |
| | <span style="color:red">leash15</span> | <span style="color:red">GGTCATAGCCCCCTTATTAGCGTTTGCCATCT</span> |
| | <span style="color:red">leash16</span> | <span style="color:red">TTTCATAATCAAAATCACCGGAACCAGAGCCA</span> |
| | <span style="color:red">leash17</span> | <span style="color:red">CCACCGGAACCGCCTCCCTCAGAGCCGCCACC</span> |
| | <span style="color:red">leash18</span> | <span style="color:red">CTCAGAACCGCCACCCTCAGAGCCACCACCCT</span> |
| | <span style="color:red">leash19</span> | <span style="color:red">CAGAGCCGCCACCAGAACCACCACCAGAGCCG</span> |
| | <span style="color:red">leash20</span> | <span style="color:red">CCGCCAGCATTGACAGGAGGTTGAGGCAGGTC</span> |
| | <span style="color:red">leash21</span> | <span style="color:red">AGACGATTGGCCTTGATATTCACAAACAAATA</span> |
| | <span style="color:red">leash22</span> | <span style="color:red">AATCCTCATTAAAGCCAGAATGGAAAGCGCAG</span> |
| | <span style="color:red">leash23</span> | <span style="color:red">TCTCTGAATTTACCGTTCCAGTAAGCGTCATA</span> |
| | <span style="color:red">leash24</span> | <span style="color:red">CATGGCTTTTGATGATACAGGAG</span> |

**Staple sections incorporating dye attachments:**

Guanine was avoided as terminal base to exclude fluorescence quenching of the dyes as far as possible.[10]

| Design | Modification | | Sequence (5' to 3') | Location | |
|---|---|---|---|---|---|
| Design A1 | Atto647N | 5' | AGGAAACGCAATAATAA | leash1* | |
| | Atto532 | 5' | TTGAGTTAAGCGAAGGAAACCG | 34[90] | 35[90] |
| | unmodified | | CGGAATACCCAAAAGAACTGGCA | leash2a* | |
| | unmodified | | TGATTAAGACTCCTTATTACGCAG | leash2b* | |
| | | | | | |
| Design A2 | Atto647N | 5' | AGGAAACGCAATAATAA | leash1* | |
| | Atto532 | 5' | CGGAATACCCAAAAGAACTGGCA | leash2a* | |
| | unmodified | | TGATTAAGACTCCTTATTACGCAG | leash2b* | |

## 14. Diagram of PDMS-based micro-fluidic chip.
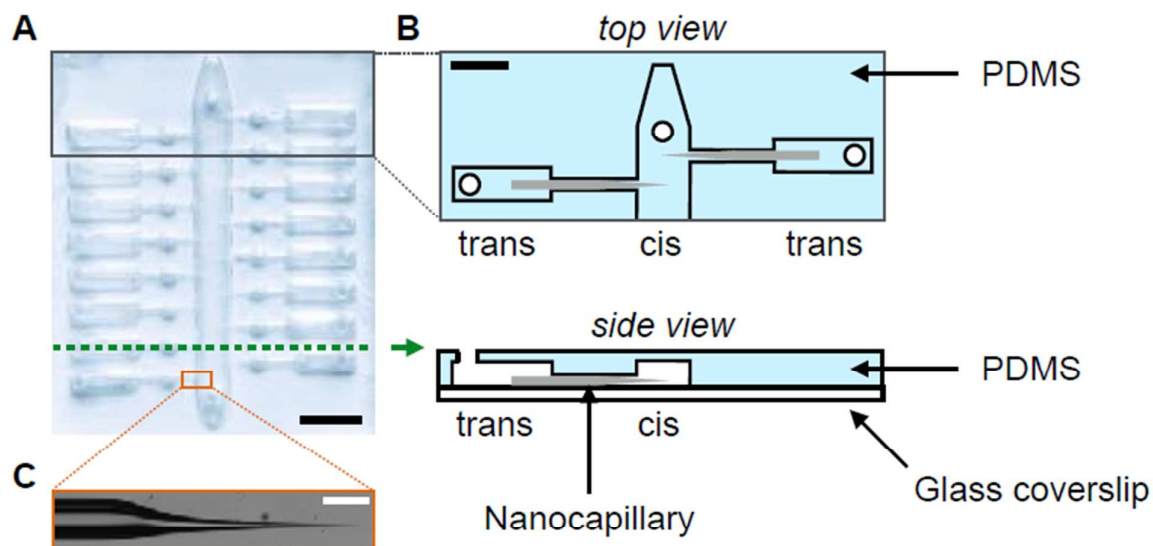


**Figure S10: A** Image of PDMS-based microfluidic device containing 16 quartz nanocapillaries. Scale bar 5 mm. **B** Zoom-in schematic of microfluidic chip as seen from top and the side. The nanocapillary connects the central *cis* reservoir to an individual *trans* reservoir. Punched holes are used to immerse Ag/AgCl electrodes. The *cis* reservoir corresponds to the electrically grounded side. Scale bar 2.5 mm. **C** Optical microscopy image of the quartz nanocapillary. Scale bar 0.5 mm.

## 15. Analysis of occurrence of single vs. multiple origami trapping events.

We are able to identify the capture of multiple DNA origami structures as (i) a larger conductance drop $\Delta G$ and (ii) a higher maximum fluorescence emission compared to a single DNA origami plate at a given voltage. In two earlier publications (see Hernández-Ainsa et al. *Nano Letters* 14.3 (2014): 1270-1274[5] and Hernández-Ainsa et al. ACS nano 7.7 (2013) : 6024-6030)[11] we carefully analysed the intrinsic variability in absolute fluorescence intensities among different capture events and capillaries including the plastic deformation of DNA origami structures with a leash.

We performed the following experiment to prove single capture of DNA origami structures:

DNA origami plates were assembled that are labelled with a single dye, either with a donor (ATTO532) or acceptor (ATTO647N), using the predefined dye positions in design $A_1$. After folding and filtering, the two samples were mixed in an equimolar ratio and the measurements were performed at a low, constant voltage of 200 mV. Both fluorescence channels ($I_D(D^*)$ and $I_A(A^*)$) were constantly monitored during every DNA origami insertion, as shown in Figure 1. In the simplest case of capturing two DNA origami structures on the nanocapillary tip, we would expect a 50% fraction of two-colour and a 50% fraction of single-colour fluorescence signals. In contrast, 98% of the DNA origami capture events ($N$=101) show only one fluorescence signal (Figure S12). The absence of partially overlapping signals in the $I_D(D^*)$ and $I_A(A^*)$ channels indicates that the formation of aggregates after mixing of the two samples is extremely unlikely.

The occurrence of aggregates forming during the folding and purification process (i.e. before mixing of the two species) is low at 7%, as estimated from the relative band intensities using agarose gel electrophoresis (Figure S13).
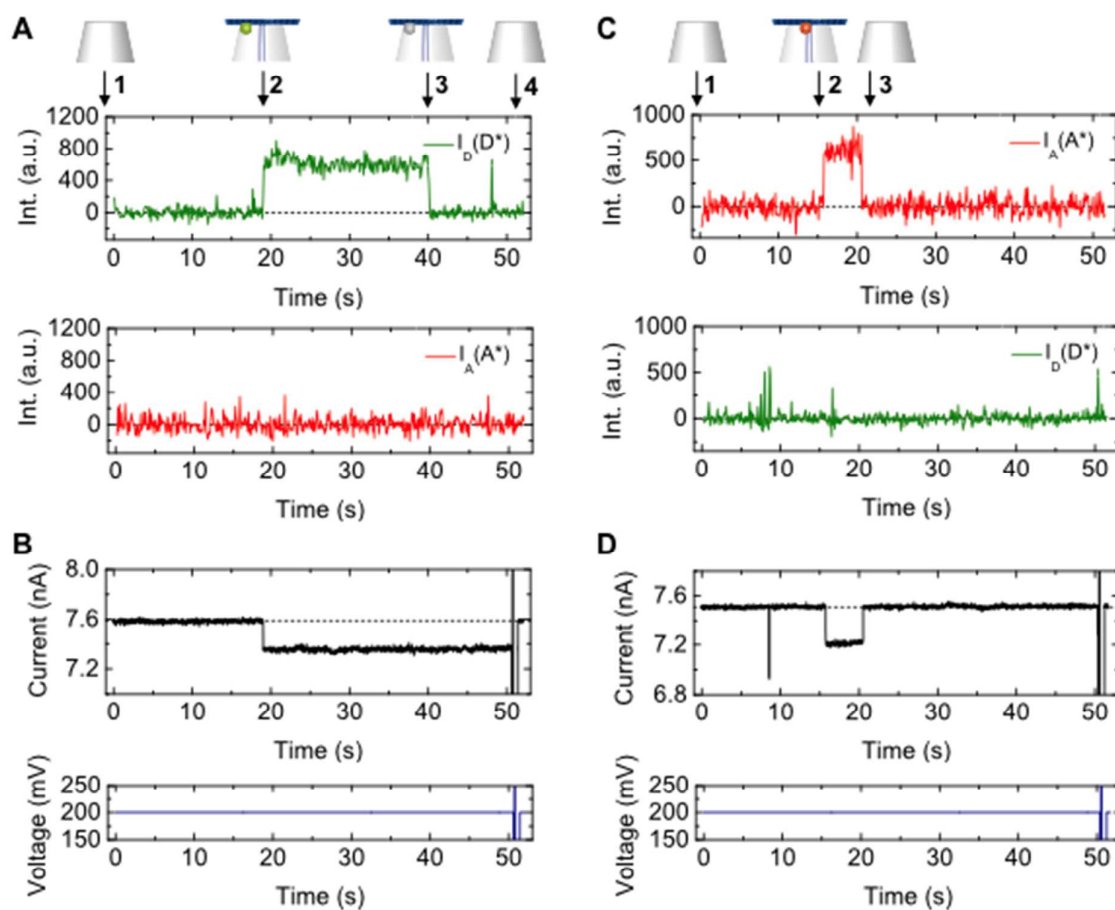
**Figure S12.** Representative examples of fluorescence intensity traces correlated with voltage and ionic current recordings for DNA origami plates with a single fluorescent label with dye locations as in design $A_1$. **(A)** Donor-only (ATTO532) structure. (*top*) Trace annotations: **1** Bare nanocapillary. **2** DNA origami trapping. **3** Donor bleaching. **4** DNA origami ejection. (*bottom*) Fluorescence intensity traces $I_D(D^*)$ and $I_A(A^*)$. **(B)** Ionic current and voltage traces. **(C)** Acceptor-only (ATTO647N) structure. (*top*) Trace annotations: **1** Bare nanocapillary. **2** DNA origami trapping. **3** DNA origami translocation. (*bottom*) Fluorescence intensity traces $I_A(A^*)$ and $I_D(D^*)$. **(D)** Ionic current and voltage traces.
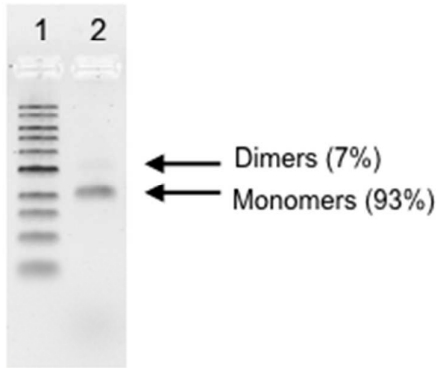
**Figure S13.** Agarose gel electrophoresis. Lane 1: 1 kb ladder. Lane 2: DNA origami plate with monomer (93%) and dimer band (7%) as measured by intensity.

**References**

(1)     van Dorp, S.; Keyser, U. F.; Dekker, N. H.; Dekker, C.; Lemay, S. G. Origin of the Electrophoretic Force on DNA in Solid-State Nanopores. *Nat. Phys.* **2009**, *5*, 347–351.

(2)     Slone, S. M.; Li, C.-Y.; Yoo, J.; Aksimentiev, A. Molecular Mechanics of DNA Bricks: In Situ Structure, Mechanical Properties and Ionic Conductivity. *New J. Phys.* **2016**, *18*, 55012.

(3)     Yoo, J.; Aksimentiev, A. Improved Parametrization of Li + , Na + , K + , and Mg 2+ Ions for All-Atom Molecular Dynamics Simulations of Nucleic Acid Systems. *J. Phys. Chem. Lett.* **2012**, *3*, 45–50.

(4)     Comer, J.; Aksimentiev, A. Predicting the DNA Sequence Dependence of Nanopore Ion Current Using Atomic-Resolution Brownian Dynamics. *J. Phys. Chem. C* **2012**, *116*, 3376–3393.

(5)     Hernández-Ainsa, S.; Misiunas, K.; Thacker, V. V.; Hemmig, E. A.; Keyser, U. F. Voltage-Dependent Properties of DNA Origami Nanopores. *Nano Lett.* **2014**, *14*, 1270–1274.

(6)     Laohakunakorn, N.; Ghosal, S.; Otto, O.; Misiunas, K.; Keyser, U. F. DNA Interactions in Crowded Nanopores. *Nano Lett.* **2013**, *13*, 2798–2802.

(7)     Bustamante, C.; Smith, S. B.; Liphardt, J.; Smith, D. Single-Molecule Studies of DNA Mechanics. *Curr. Opin. Struct. Biol.* **2000**, *10*, 279–285.

(8)     Smith, S. B.; Cui, Y.; Bustamante, C. Overstretching B-DNA : The Elastic Response of Individual Double-Stranded and Single- Stranded DNA Molecules. *Science (80-. ).* **1996**, *271*, 795–799.

(9)     Keyser, U. F. Controlling Molecular Transport through Nanopores. *J. R. Soc. Interface* **2011**, *8*, 1369–1378.

(10)    Gust, A.; Zander, A.; Gietl, A.; Holzmeister, P.; Schulz, S.; Lalkens, B.; Tinnefeld, P.; Grohmann, D. A Starting Point for Fluorescence-Based Single-Molecule Measurements in Biomolecular Research. *Molecules* **2014**, *19*, 15824–15865.

(11)    Hernández-Ainsa, S.; Bell, N. A. W.; Thacker, V. V.; Göpfrich, K.; Misiunas, K.; Fuentes-Perez, M. E.; Moreno-Herrero, F.; Keyser, U. F. DNA Origami Nanopores for Controlling DNA Translocation. *ACS Nano* **2013**, *7*, 6024–6030.